Three Dimensional Constraint Effects on the Estimated ΔCTOD during the Numerical Simulation of Different Fatigue Threshold Testing Techniques

Banavara R. Seshadri*
National Institute of Aerospace, Hampton, VA 23681

and

Stephen W. Smith†
NASA Langley Research Center, Hampton, VA 23681

Variation in constraint through the thickness of a specimen effects the cyclic crack-tip-opening displacement (ΔCTOD). ΔCTOD is a valuable measure of crack growth behavior, indicating closure development, constraint variations and load history effects. Fatigue loading with a continual load reduction was used to simulate the load history associated with fatigue crack growth threshold measurements. The constraint effect on the estimated ΔCTOD is studied by carrying out three-dimensional elastic-plastic finite element simulations. The analysis involves numerical simulation of different standard fatigue threshold test schemes to determine how each test scheme affects ΔCTOD. The American Society for Testing and Materials (ASTM) prescribes standard load reduction procedures for threshold testing using either the constant stress ratio (R) or constant maximum stress intensity (K_{max}) methods. Different specimen types defined in the standard, namely the compact tension, C(T), and middle cracked tension, M(T), specimens were used in this simulation. The threshold simulations were conducted with different initial K_{max} values to study its effect on estimated ΔCTOD. During each simulation, the ΔCTOD was estimated at every load increment during the load reduction procedure. Previous numerical simulation results indicate that the constant R load reduction method generates a plastic wake resulting in remote crack closure during unloading. Upon reloading, this remote contact location was observed to remain in contact well after the crack tip was fully open. The final region to "open" is located at the point at which the load reduction was initiated and at the free surface of the specimen. However, simulations carried out using the constant K_{max} load reduction procedure did not indicate remote crack closure. Previous analysis results using various starting K_{max} values and different load reduction rates have indicated ΔCTOD is independent of specimen size. A study of the effect of specimen thickness and geometry on the measured ΔCTOD for various load reduction procedures and its implication in the estimation of fatigue crack growth threshold values is discussed.

Nomenclature

a_i	=	initial crack length
a	=	crack length
B	=	thickness of the specimen
C	=	stress intensity gradient, K-gradient
da	=	crack tip element size
E	=	Young's modulus
K_{max}	=	maximum stress intensity factor
K_{min}	=	minimum stress intensity factor
P	=	applied pin load for C(T) specimen
R	=	stress ratio, load ratio
S	=	applied stress for M(T) specimen
x,y,z	=	coordinates in x,y and z direction
Δa	=	crack growth increment
$\Delta CTOD$	=	cyclic crack-tip-opening displacement
ΔK	=	applied stress intensity factor range

* Senior Research Scientist, 100 Exploration Way, Member AIAA
† Senior Materials Engineer, Durability, Damage Tolerance and Reliability Branch, MS 188E

ΔK_o = initial stress intensity factor range
ΔK_{th} = fatigue threshold stress intensity factor level
$K_{max(o)}$ = initial maximum stress intensity factor
σ_o = flow stress

I. Introduction

The fatigue threshold stress intensity factor level, ΔK_{th}, defines the stress intensity range, ΔK, at which a crack in metallic materials will arrest or begin to propagate. The threshold is used in the aerospace industry to define a durability lifetime (or safe operating time) for many components[1]. Therefore, accurate threshold data is critical to the safety of durability-based designs. The development of fatigue crack growth threshold data is standardized within organizations such as The American Society for Testing and Materials (ASTM) and International Standards Organization (ISO). The standards outline the experimental procedure, specimen geometry, and crack configurations along with tolerances on dimensions and operating parameters. The fatigue crack growth threshold, ΔK_{th}, for large cracks is determined by gradually reducing the stress intensity factor range applied during a fatigue crack growth test until a fatigue crack growth rate of 10^{-10} m/cycle is achieved. This reducing stress intensity factor method results in a decreasing applied load as the test is performed, therefore, the process is known as a load reduction method. It should be noted that the rate of 10^{-10} m/cycle is arbitrarily chosen as a value where the fatigue crack growth rate curve is nearly vertical for most materials, indicating a "threshold".

The ASTM Standard Test Method for Measurement of Fatigue Crack Growth Rates (E647)[‡] recommends that the stress, or load, ratio (R) be held constant during the required load reduction procedure to generate threshold data. The constant R load reduction procedure is shown schematically in Figure 1.a, where both the maximum stress intensity factor, K_{max} and the minimum stress intensity factor, $K_{min,}$ are shown to decrease monotonically such that their ratio ($R=K_{min}/K_{max}$) is held constant. Experimental evidence suggests that the constant R load reduction procedure can result in the development of closure levels greater than the steady-state value[2-3], which can influence the growth rate. A constant R load reduction results in larger plastic strains along the crack wake, created from high loads early in the test procedure, with subsequently reducing loads near threshold. The larger plastic strain away from the crack tip may result in contact of the plastic wake surfaces away from the crack tip during the unloading portion of the fatigue cycle, resulting in remote crack closure (Fig.1.b). In an attempt to avoid plasticity-induced crack closure along the crack wake as the threshold is approached, an alternative load reduction procedure has been adopted, in which the maximum stress intensity factor, K_{max}, is held constant (Fig.1.a). In this technique, K_{max} is held constant while increasing K_{min}. thereby continually increasing R such that threshold measurements are made in the absence of crack closure. The resulting effective threshold stress intensity $(\Delta K_{eff})_{th}$ is often referred to as an intrinsic measurement of fatigue crack growth resistance[3-6].

Two-dimensional plane stress analyses of the effects of load reduction on fatigue crack growth were conducted by McClung[7], using both the finite element method[7-8] and a modified strip-yield model[8]. The load reduction procedure examined was limited to the constant R method. McClung observed elevated crack opening stresses as determined by the finite element analyses during the load reduction procedure. Two-dimensional analyses conducted by Newman[9] using a modified strip-yield model that averaged three-dimensional constraint effects through the thickness using an empirical constraint factor indicated that remote crack closure away from the crack tip can occur for a constant R load reduction procedure. This remote crack closure results in the crack tip opening prior to regions remote to the crack tip during loading. These elevated opening stress values would in turn lead to increased or non-conservative ΔK_{th} values. Daniewicz, et al.[10] simulated both constant R and constant K_{max} load reduction procedures using three-dimensional elastic-plastic finite element analyses. The three-dimensional analyses allow for a more realistic perspective of the plastic wake and subsequent crack opening behavior. However, the analysis was limited to large initial ΔK values, and the load reduction was confined to a few cycles due to computational limitations. Therefore, the value of ΔK_{th} was not reached during the load reduction procedure simulation.

The parameter, ΔCTOD is considered to be a fundamental parameter to characterize crack-tip damage[11-12]. To asses crack tip damage, Newman[11] evaluated ΔCTOD for the M(T) specimen subjected to various constant amplitude loading conditions. Newman considered only the plastic contribution to cyclic crack-tip displacement and neglected the elastic contribution leading to a variation in the results for different

[‡] ASTM E647-05, Standard Test Methods for Measurement of Fatigue Crack Growth Rates

stress ratios. Similarly, Bichler and Pippan[12] made experimental observations of residual plastic deformation near the crack tip (residual CTOD) to explain the overload effects on the fatigue crack growth rate. Using various starting K_{max} values and different load reduction rates, Seshadri, et al.[13-14] have shown that ΔCTOD is independent of specimen width. The estimated ΔCTOD values along a crack wake can be used to provide insight on the remote crack closure phenomenon (Fig.1.a) predicted for the constant R load reduction technique. Also, for the constant K_{max} load reduction procedure, ΔCTOD values indicate that no closure is present throughout the loading.

The main objective of this paper is to determine the constraint effects on ΔCTOD by numerically modeling fatigue crack growth in M(T) and C(T) specimens subjected to different load reduction testing procedures. The effect of thickness on estimated ΔCTOD, crack closure level and its implications on near threshold processes will be investigated.

II. Finite Element Analyses

Numerical studies have been carried out using three-dimensional elastic-plastic finite element analyses to model plasticity-induced crack closure under cyclic loading[8,10,13-15] Seshadri, et al.[16-17] have performed analyses with through and part-through cracks for the estimation of crack closure levels through the specimen thickness under constant amplitude loading, and various load reduction procedures, and have studied the effects of load history using three-dimensional elastic-plastic finite element analysis. Because of the very small element sizes required for mesh convergence, three-dimensional finite element analysis of plasticity-induced closure present a very computationally intensive effort. To obtain converged solutions, a minimum requirement is that 5-10 elements are contained within the plastic zone at any point on the crack front under the maximum loading[8, 16-17]. Crack closure and ΔCTOD estimates are made by monitoring nodal displacements during both the loading and unloading portions of cyclic loading[13-14]. The estimates are made at both "local" and "remote" locations. The "local" location represents a material point very close to the crack tip which characterizes the local crack tip region. The remote location corresponds to an initial crack tip location where earlier experimental evidence suggests that crack closure occurs under a constant R load reduction procedure[2-3]. Crack growth under cyclic loading is then simulated by loading the model with the maximum stress level of interest, and then releasing the nodes along the crack front to increase the crack size by one element.

C(T) and M(T) specimens, as shown in Figure 2, exhibited two and three planes of symmetry, respectively, and consequently only one fourth and one eighth of the geometries were modeled using eight-node brick elements. Both the specimens were of 76.2 mm width and thicknesses , B of 12.7 and 2.54 mm were examined. The C(T) model consisted of a total of 43,752 nodes and 27,722 elements. The M(T) specimen model consisted of 38,712 nodes and 24,530 elements. Both specimens were analyzed using the ZIP3D[18] finite element code. A typical ZIP3D finite element model of the C(T) specimen is shown in Figure 3. The length of the crack tip elements was on the order of 10 microns. The aluminium alloy 7075-T73 was considered throughout the analyses, and it has a bi-linear behavior with modulus E = 71.0 GPa and flow stress σ_o = 400 MPa. The von Mises yield criterion and the associated flow rule were used. Small deformation theory was employed. The crack front was advanced one element during each cycle such that da = 10 microns. Load cycles were applied to simulate load reduction in the range of ΔK of 20 MPa√m to 1 MPa√m under both constant R and constant K_{max} load reduction procedures.

The load reduction used was defined with the following relationship:

$$\Delta K = \Delta K_o e^{C\Delta a} \qquad (1)$$

where, Δa is the amount of crack growth during load reduction, ΔK_o is the initial stress intensity factor range at the start of load reduction, and C (K-gradient) is a constant. For the constant R load reduction case, a value of R = 0.1 was used, with initial cyclic stress intensity levels, ΔK_o, of 20, 15 and 10 MPa√m. For the constant K_{max} load reduction case, values of K_{max} = 22.2, 16.7 and 11.1 MPa√m were considered, with an initial value of R = 0.1, resulting in the same initial ΔK values used for the constant R case. The first few load cycles were used to simulate constant amplitude pre-cracking with $\Delta K = \Delta K_o$ and R = 0.1. The remaining load cycles were used to simulate the load reduction procedures. The schematic representation of different load reduction procedures simulated in the current study is shown in Figure 1. The load reduction analyses presented are for a C of -500 m^{-1}. While this is a greater K-gradient than prescribed for constant R load reduction in ASTM standard E 647 (-80 m^{-1}), this rate was necessary to maintain practical computational requirements.

III. Results and Discussions

The variations in local ΔCTOD and crack closure levels for a C(T) specimen under the constant R=0.1 load reduction procedure with an initial ΔK_o of 15 MPa√m are shown in Figure 4. The local closure and ΔCTOD values are calculated at one node, or 10 microns, behind the current crack tip location. The estimated ΔCTOD values through the thickness decrease with decreasing ΔK during the constant R load reduction procedure. At higher applied ΔK, ΔCTOD is observed to vary through the thickness as shown in Figure 4, where the solid black lines indicate values computed at the outer surface and dashed black lines indicate values computed at the mid-plane. However, as the applied ΔK value decreases below a value of approximately 5 MPa√m, the variation in ΔCTOD through the thickness is negligible. During this load reduction, local crack closure levels on the outer surface decrease from the steady state value of 0.38 computed at the initial ΔK_o of 15 MPa√m. For applied ΔK values less than 7 MPa√m, locally, the crack remains fully open through the thickness of the specimen (see solid and dashed red lines in Fig.4). With further reduction in applied ΔK to the near threshold regime, the estimated ΔCTOD value decreases while the crack remains fully open locally.

The comparisons of remote ΔCTOD and crack closure level for the constant R and constant K_{max} load reduction procedures are shown in Figure 5. The analysis of the C(T) specimen was performed with an initial ΔK_o value of 15 MPa√m. In Figure 5, variations in remote ΔCTOD for two different through-the-thickness locations are provided for constant R (solid and dashed black lines in Fig.5) and constant K_{max} (dash-dot and dashed blue lines in Fig.5) load reduction procedures. Remote crack closure levels for the constant R load reduction procedure (solid and dashed red lines in Fig.5) are also provided. For the constant K_{max} load reduction procedure, the crack remains fully open. No crack closure is observed for the constant R test for applied ΔK greater than 7 MPa√m; however, closure is observed to increase with decreasing ΔK. The initial closure is observed on the surface of the specimen (z = 6.35 mm) and closure at the mid-plane of the specimen is not observed until the applied ΔK approaches 4 MPa√m. While the general trend observed in Figure 5 for ΔCTOD is nearly the same for the constant R and constant K_{max} load reduction procedures, the ΔCTOD values are greater for the K_{max} procedure compared to the constant R load reduction data, particularly for applied ΔK less than 7 MPa√m.

Earlier experimental[2-3] results have shown the existence of remote crack closure on the outer surface at higher initial ΔK_o values during the constant R load reduction procedure. To understand the extent of crack closure at a remote location, several nodal points were chosen on the outer surface and the closure levels were computed during the constant R load reduction procedure. Here, the remote location corresponds to a nodal point close to the initial crack tip (a_i/W=0.264) just before the commencement of the load reduction procedure. The variations in remote crack closure levels corresponding to these remote nodal points for an M(T) specimen are depicted in Figure 6. The variation in crack closure levels at different remote locations versus applied ΔK is represented in Figure 6. The nodal location corresponding to the x=0.0 mm location in the figure corresponds to the beginning of the load reduction procedure (a_i/W=0.264). The nodal points ahead of the reference point are indicated by positive x-coordinates, and the locations behind are indicated by negative x-coordinates. The crack closure level at remote locations steadily increases as the applied ΔK is decreased. A closure value of nearly one is obtained in the fatigue threshold regime; indicating the remote region (range of 200 microns) remained closed throughout the load cycle. From Figure 6, remote crack closure is suggested by the variation in closure for applied ΔK from approximately 19 to 10 MPa√m. As the remote closure level increases with decreasing ΔK, the local closure level decreases (solid black line in Fig.6). For this simulation, the crack remains fully open locally (as indicated by the local closure level being equal to the applied R, 0.1) in the threshold regime and closure occurs at a remote location. Due to remote crack closure phenomenon observed under the constant R load reduction procedure, the local load at the crack tip will depend on the applied initial ΔK_o value and load reduction constant, C.

A. Effect of specimen type

Comparison of local ΔCTOD and crack closure levels for M(T) and C(T) specimens under a constant load reduction procedure are shown in Figure 7. The comparison is made for the constant R load reduction procedure with an initial ΔK_o of 10 MPa√m for both specimen types. Here, local ΔCTOD and crack closure levels are shown for two different through-the-thickness locations for both the M(T) (solid and dashed black lines in Fig.7) and C(T) (dash-dot and dashed blue lines in Fig.7) specimens. Similar trends of decreasing ΔCTOD with decreasing ΔK and increasing ΔCTOD from the outer surface to the mid-plane are observed for both specimen types. The variation of the estimated ΔCTOD through the thickness is greater for the C(T)

specimen than is observed for the M(T) specimen, particularly at higher values of applied ΔK. Here, the ΔCTOD values at Z=6.35 mm and Z=0.0 mm for the M(T) specimen are bound by the values for the C(T) specimen at the same two locations. For the initial portion of the constant R load reduction procedure (higher ΔK), the M(T) specimen (solid and dashed red lines in Fig.7) exhibits a higher local crack closure level through the thickness when compared to the C(T) (dash-dot and dashed green lines in Fig.7) specimen. As the applied ΔK becomes less than 6 MPa√m, the crack remains fully open locally for both specimen types.

B. Effect of specimen thickness

Numerical simulations of different load reduction procedures for both C(T) and M(T) specimens were carried out to understand the effects of specimen thickness on estimated ΔCTOD. Specimen thickness directly influences the calculated fatigue threshold level for various thickness specimens tested under different load reduction procedures[19]. The study was aimed at understanding and explaining the effects of plasticity associated with specimens of different thickness. Even though simulations were carried out for both C(T) and M(T) specimens, the results pertaining to only C(T) specimens will be discussed. Similar behavior and trends were observed for the M(T) specimen. A comparison of variations in local ΔCTOD with applied constant R load reduction procedure for two thicknesses are shown in Figure 8. The thicknesses examined were B = 12.7 and 2.54 mm, representing thick and thin specimen configuration sizes, respectively. The simulations were carried out under identical conditions i.e., same initial applied ΔK_o, stress ratio R, K-gradient C and the crack tip element size. In general, the thin specimen is under the state of a plane stress condition compared to the thick specimen. This leads to an increase in plastic zone size on the outer surface of the thin specimen. In Figure 8, variations in ΔCTOD and local crack closure level during the constant R load reduction procedure simulation are presented for two specimen thicknesses. Due to the large plastic zone size on the outer surface (Z/B=1.0), the thin specimen experiences a higher crack closure level (solid and dashed red lines in Fig.8) and decreased estimated ΔCTOD (solid and dashed black lines in Fig. 8) values compared to the thick specimen (dash-dot and dashed green and blue lines respectively in Fig.8). In the interior region, (Z/B= 0.0) there is little difference between estimated ΔCTOD and local crack closure levels for thin and thick specimens. As the applied ΔK is reduced below 7 MPa√m, the crack remains fully open locally, and the estimates of ΔCTOD for both specimens are nearly identical.

The comparisons of remote ΔCTOD and crack closure level for two different thickness specimens for a constant load reduction procedure are shown in Figure 9. The analysis of the C(T) specimen was performed with an initial ΔK_o value of 15 MPa√m. As before, variations in remote ΔCTOD and closure levels are presented for the two different thickness specimens. The thin specimen (solid and dashed red lines in Fig.9) experiences higher closure levels than the thick (dash-dot and dashed green lines in Fig.9) specimen. Additionally, the estimated ΔCTOD is much lower for the thin specimen (solid and dashed black lines in Fig.9) than for the thick specimen (dashed-dot and dashed blue lines in Fig.9). The difference in estimated ΔCTOD between the thin and thick specimen is dependent upon the applied ΔK_o value. The maximum crack closure level reaches a value of 0.76 on the outer surface at the remote location for the thin specimen. For the thick specimen, the estimated maximum closure level is approximately 0.34. The higher the value of applied ΔK_o, the greater the amount of plasticity produced for the thin specimen, which in turn leads to higher closure level at the remote location. Also, there is a slight variation in the estimated remote ΔCTOD and crack closure level through the thickness for both thin and thick specimens.

The variations in closure level at several remote nodal points close to the initial crack tip just before the commencement of a load reduction procedure for both thin and thick specimens are shown in Figure 10. The nodal coordinates and their location with respect to the initial crack tip were previously described during the discussion of Figure 6. The nodal location corresponding to the x=0.0 mm location in the figure corresponds to the beginning of the load reduction procedure (a_i/W=0.263). The nodal points ahead of the reference point are indicated by positive x-coordinates, and the locations behind are indicated by negative x-coordinates. All of these nodal points are located on the outer surface. For both thin and thick specimens, the remote closure level steadily increases as the applied ΔK is decreased. Due to the large plastic zone size associated with the thin specimens, thin specimens experience a higher closure level when compared to thick specimens as the threshold is approached.

The amount of remote closure is dependent upon the applied initial ΔK_o value. If the applied initial ΔK_o value is much higher than the current value, one might expect closure levels nearly approaching one as the

fatigue threshold is approached, which is similar to the case shown in Figure 6. For completeness, the variation in local closure level with decreasing applied ΔK is shown for the thin (solid black line) and thick (solid green line) specimens in Figure 10. As the applied ΔK approaches the fatigue threshold regime, locally the crack tip remains fully open for each specimen. However, at various remote locations, the closure level steadily increases as the applied ΔK is decreased in the fatigue threshold regime.

Concluding Remarks

Numerical estimates of ΔCTOD were carried out using three-dimensional elastic-plastic finite element analyses for both M(T) and C(T) specimens. The constant R and constant K_{max} load reduction procedures were simulated to study load history effects on the fatigue crack growth threshold. Due to computational limitations, the analyses were performed for C = -500 m^{-1} for all load reduction methods, which is more than 6 times greater than that prescribed for the constant R load reduction method. The following conclusions were made from the analyses.

- The analyses confirmed the existence of remote, three-dimensional crack closure for both M(T) and C(T) specimens under the constant R load reduction procedure detailed in this study.
- The analyses also indicated that the amount of remote crack closure estimated in the near threshold regime is primarily dependent upon the initial value of ΔK_o chosen for the constant R load reduction procedure. In contrast, under the constant K_{max} loading, no crack closure was observed in the threshold regime.
- The local ΔCTOD computed for the M(T) specimen are bound by the values for the C(T) specimen.
- The effect of thickness on the estimated ΔCTOD and remote closure levels in the fatigue threshold regime were studied and a higher closure level is observed for specimens of reduced thickness. Here, closure is dominated by plasticity at the outer surface of the specimen.
- The results indicate that, ΔCTOD is an excellent parameter to describe differences in the crack growth behavior observed in the laboratory based on load reduction methods and specimen configuration.

References

[1] Lincoln, J.W., *Proceedings of 13th Symposium of the International Committee on Aeronautical Fatigue,* 1985.

[2]Donald, J. K. and Paris, P. C., "An Evaluation of K Estimation Procedures on 6061-T6 and 2024-T3 Aluminium Alloys," *Proceedings of Fatigue Damage of Structural Materials II,* 1998.

[3]Minakawa, K., Newman Jr., J. C., and McEvily, A. J., "A Critical Study of the Closure Effect on Near-Threshold Fatigue Crack Growth," *Fatigue and Fracture of Engineering Materials and Structures,* Vol. 6, 1983, pp. 359-365.

[4]Forth, S.C. Newman, Jr. J.C. and Forman, F.G., "On Generating Fatigue Growth Thresholds," *International Journal of Fatigue,* Vol. 25, 2003, pp. 9-15.

[5]Smith, S.W. and Piascik R.S., "An Indirect Technique for Determining Closure-Free Fatigue Crack Growth Behavior," *Fatigue Crack Growth Thresholds, Endurance Limits and Design, ASTM STP 1372*, 2000, pp. 109-122.

[6]Herman, W.A., Hertzberg, R.W. and Jaccard R.A., "A Simplified Laboratory Approach for the Prediction of Short Crack Behavior in Engineering Structures," *Fatigue and Fracture of Engineering Materials and Structures,* Vol. 11, 1998, pp. 303-320.

[7]McClung, R. C., "Finite Element Analysis of Fatigue Crack Closure: A Historical and Critical Review," *Fatigue 99, Seventh International Fatigue Conference,* China, 1999.

[8]McClung, R. C., "Analysis of Fatigue Crack Closure During Simulated Threshold Testing," *Fatigue Crack Growth Thresholds, Endurance Limits, and Design, ASTM STP 1372*, 1999, pp. 209-226.

[9]Newman Jr., J. C., "An Analysis of Fatigue Crack Growth and Closure Near Threshold Conditions for Long-Crack Behavior," *Fatigue Crack Growth Thresholds and Endurance Limits, and Design, ASTM STP 1372,* 1999, pp. 227-251.

[10]Daniewicz, S. R., and Skinner, S. D., "Finite Element Analysis of Fatigue Crack Growth Threshold Testing Techniques," *13th European Conference on Fracture, (ECF13),* San Sebastian, Spain, 2000.

[11]Newman Jr., J. C., "An Evaluation of Plasticity Induced Crack Closure Concept and Measurement Methods," *Advances in Fatigue Crack Closure Measurement and Analysis: Second Volume, ASTM 1343,* American Society for Testing and Materials, 1999, pp. 128-144.

[12]Bichler, C. and Pippan, R., "Direct Observation of the Residual Plastic Deformation Caused by a Single Tensile Overload," *Advances in Fatigue Crack Closure Measurement and Analysis: Second Volume, ASTM 1343,* American Society for Testing and Materials, 1999, pp. 191-206.

[13]Seshadri, B.R. and Forth, S.C., "Finite Element Simulation and Estimation of Cyclic Crack Tip Opening Displacement for Different Specimens During Fatigue Threshold Testing," *5th International ASTM/ESIS Symposium on Fatigue and Fracture Mechanics (35th ASTM National Symposium on Fatigue and Fracture Mechanics),* May 16-19, 2005, Reno, Nevada.

[14]Seshadri, B.R. and Forth, S.C., "Numerical Simulation and Evaluation of Different Fatigue Threshold Testing Techniques," *9th International Fatigue Congress, Fatigue 2006,* May 14-19 2006, Atlanta, Georgia.
[15]Chermahini, R. G., Shivakumar, K. N., and Newman Jr., J. C., "Three Dimensional Finite Element Simulation of Fatigue Crack Growth and Closure," *Mechanics of Fatigue Crack Closure, ASTM STP 982*, American Society for Testing and Materials, 1988, pp. 398-413.
[16]Seshadri, B.R., Dattaguru, B., and Ramamurthy, T. S., "Three Dimensional Elastic-Plastic Finite Element Analysis of Crack Closure in C(T) Specimen," *Contemporary Research in Engineering Science,* Berlin, 1995, pp. 491-515.
[17]Seshadri, B.R., *Numerical Simulation and Experimental Correlation of Fatigue Crack Closure Phenomenon under Cyclic Loading,* PhD Dissertation, Dept. of Aerospace Engineering, Indian Institute of Science, India, 1996.
[18]Shivakumar, K.N. and Newman Jr., J.C., *ZIP3D- An Elastic-Plastic Finite Element Analysis Program for Cracked Bodies*, *NASA TM* 102753, 1990.
[19]Broek, D. and Schijve, J., "The Influence of Sheet Thickness on Crack Propagation," *Aircraft Engineering,* Vol. 38, No.11, 1966, pp. 31-33.

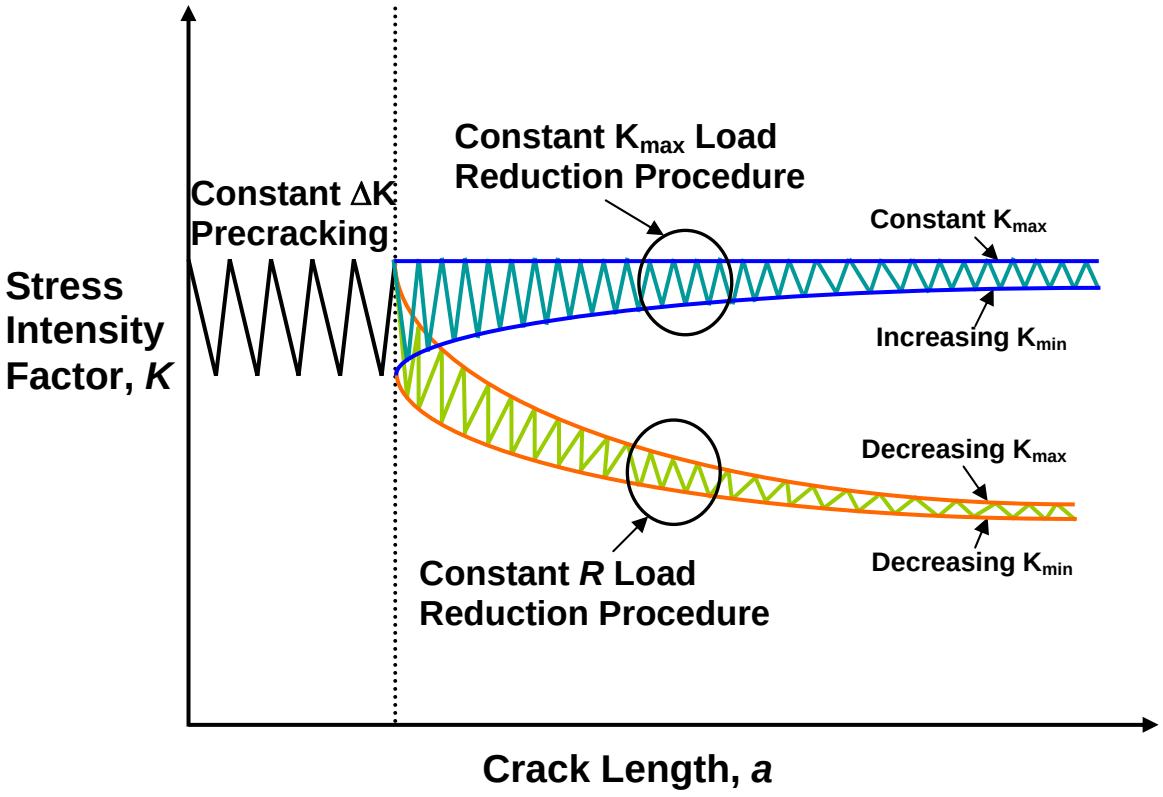

Figure 1.a A schematic representation of different experimental threshold test techniques.

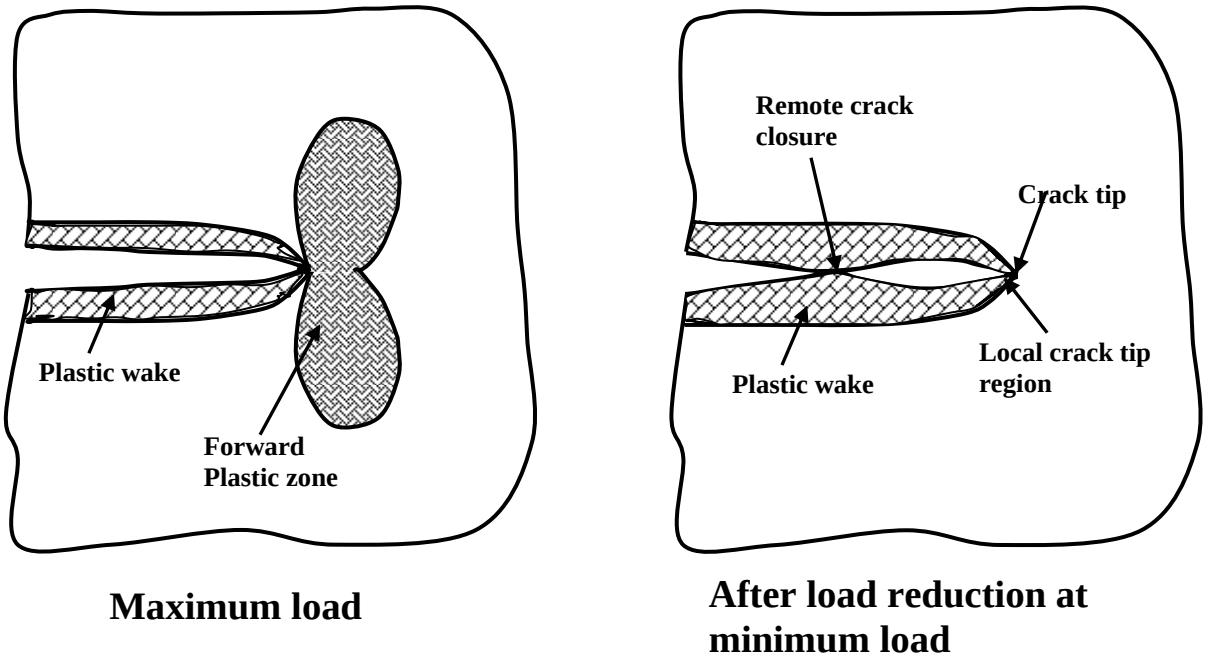

Figure 1.b Remote crack closure phenomenon observed after constant-R load reduction procedure.

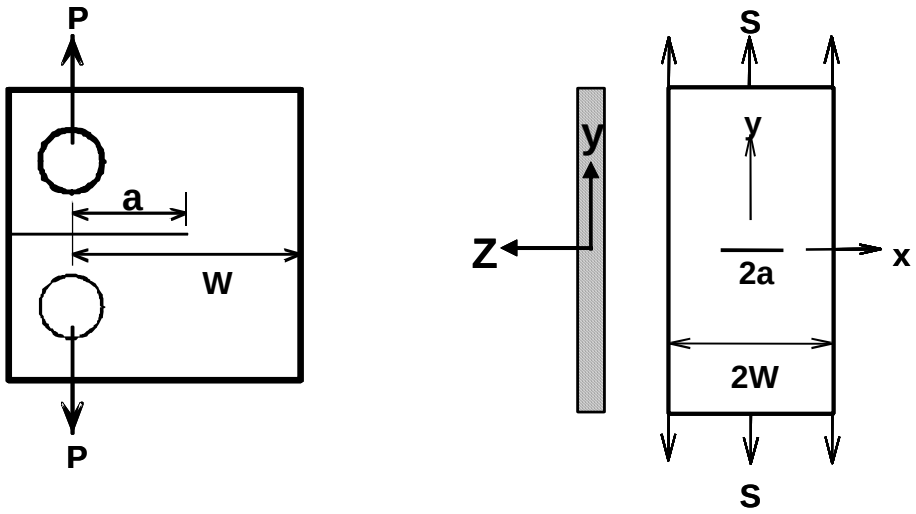

a) C(T) Specimen **b) M(T) Specimen**

Figure 2. Configurations analyzed.

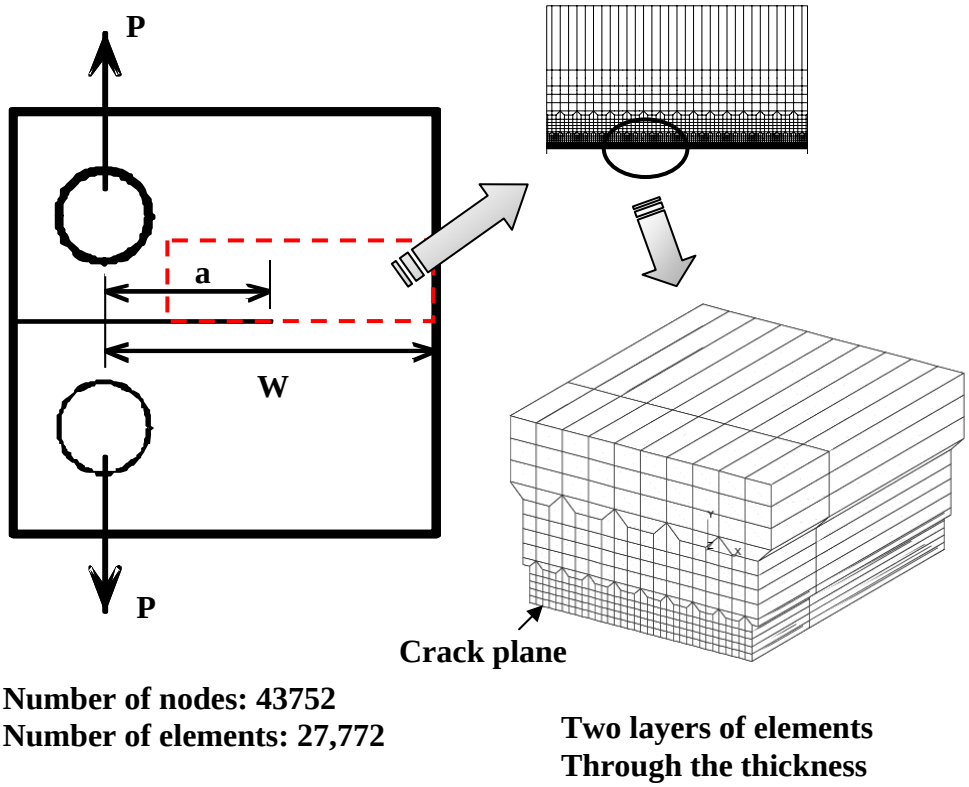

Figure 3. A typical ZIP3D finite element model of C(T) specimen.

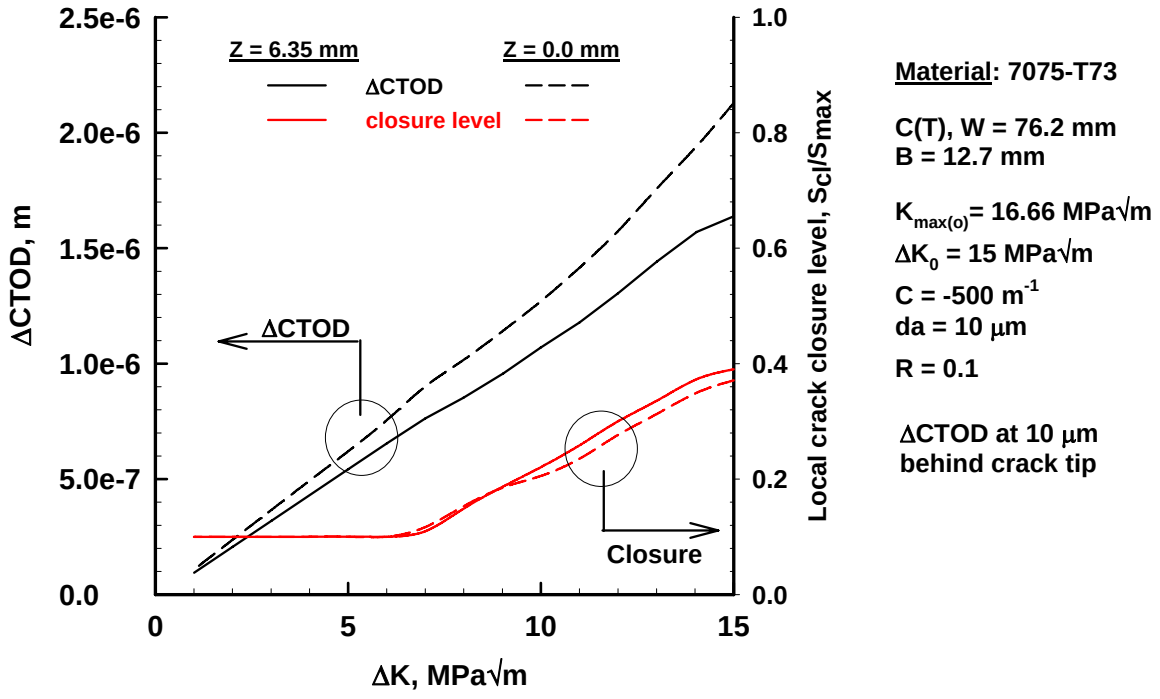

Figure 4. Variation in local ΔCTOD with applied constant R load reduction procedure at two through-thickness positions (surface (6.35 mm) and mid-plane (0.0 mm)).

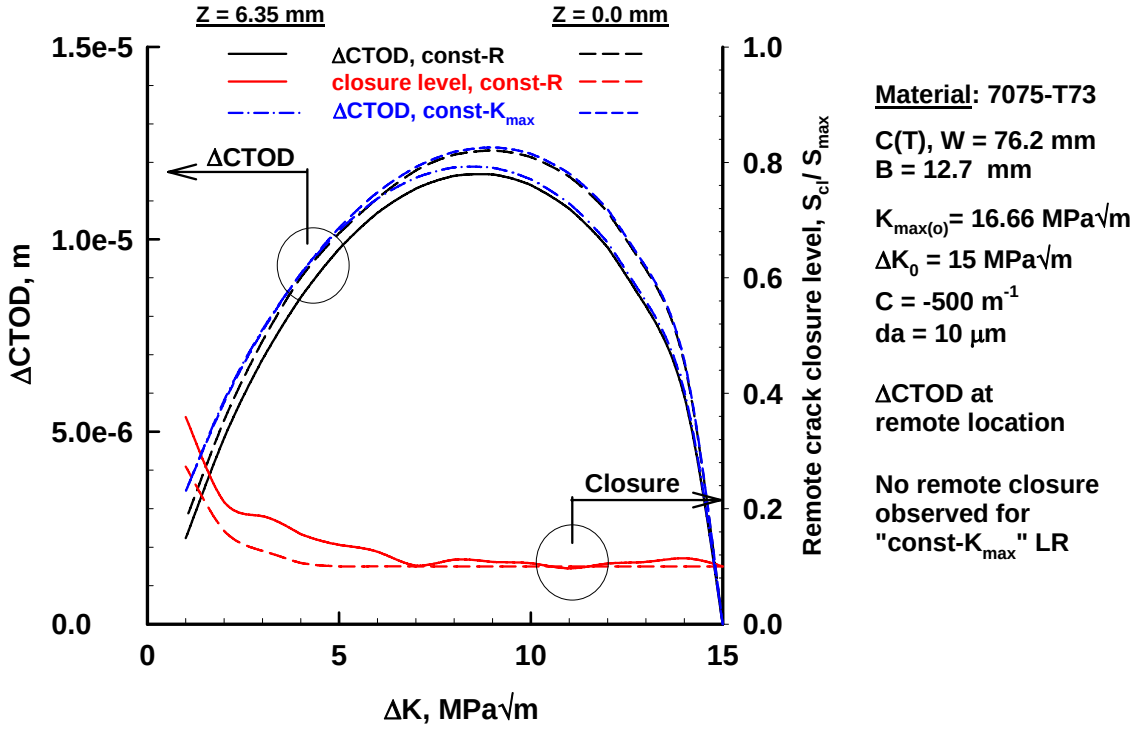

Figure 5. Comparison of remote ΔCTOD and closure level for different load reduction procedures for C(T) specimens at two through-thickness positions (surface (6.35 mm) and mid-surface (0.0 mm)).

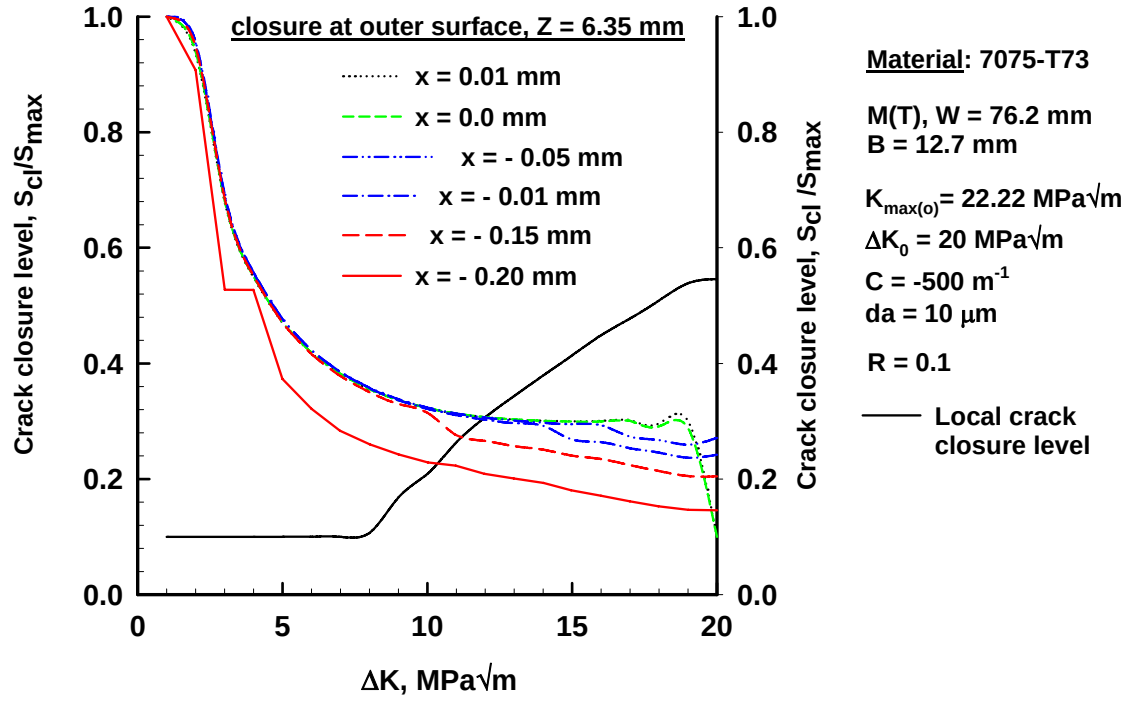

Figure 6. Variation in remote crack closure level with applied constant R load reduction procedure for ΔK$_o$ = 20 MPa√m

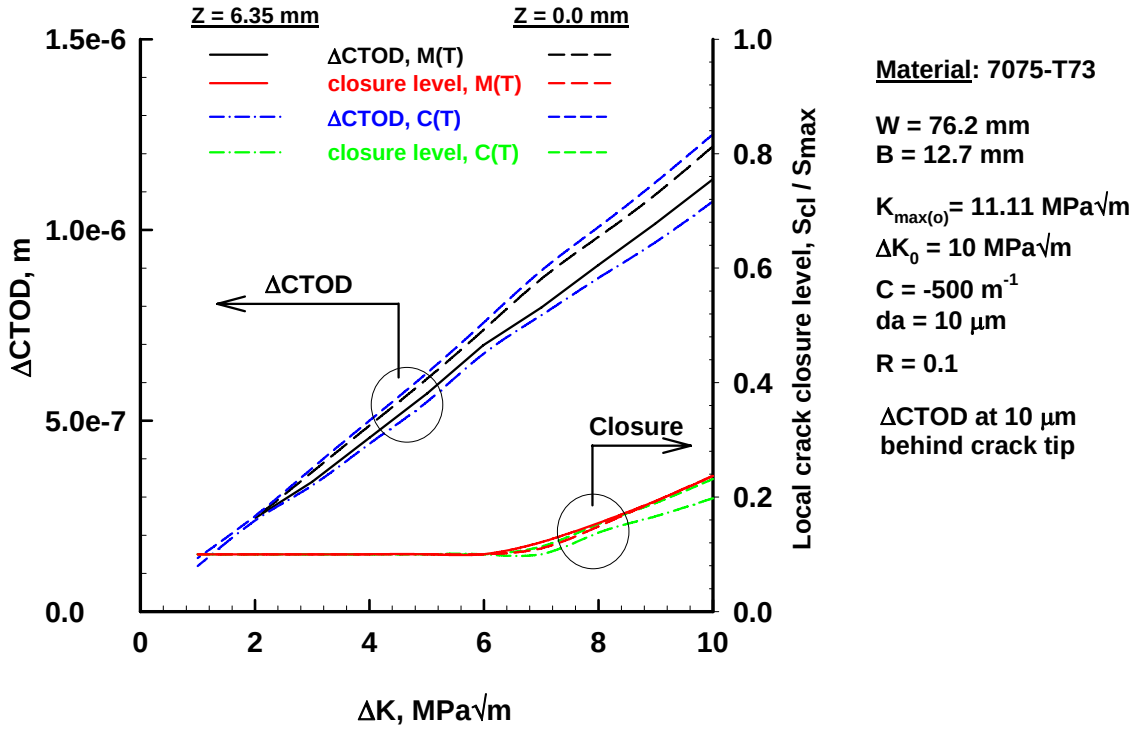

Figure 7. Comparison of variation in local ΔCTOD with applied constant R load reduction procedure for C(T) and M(T) specimens at two through-thickness positions (surface (6.35 mm) and mid-surface (0.0 mm)).

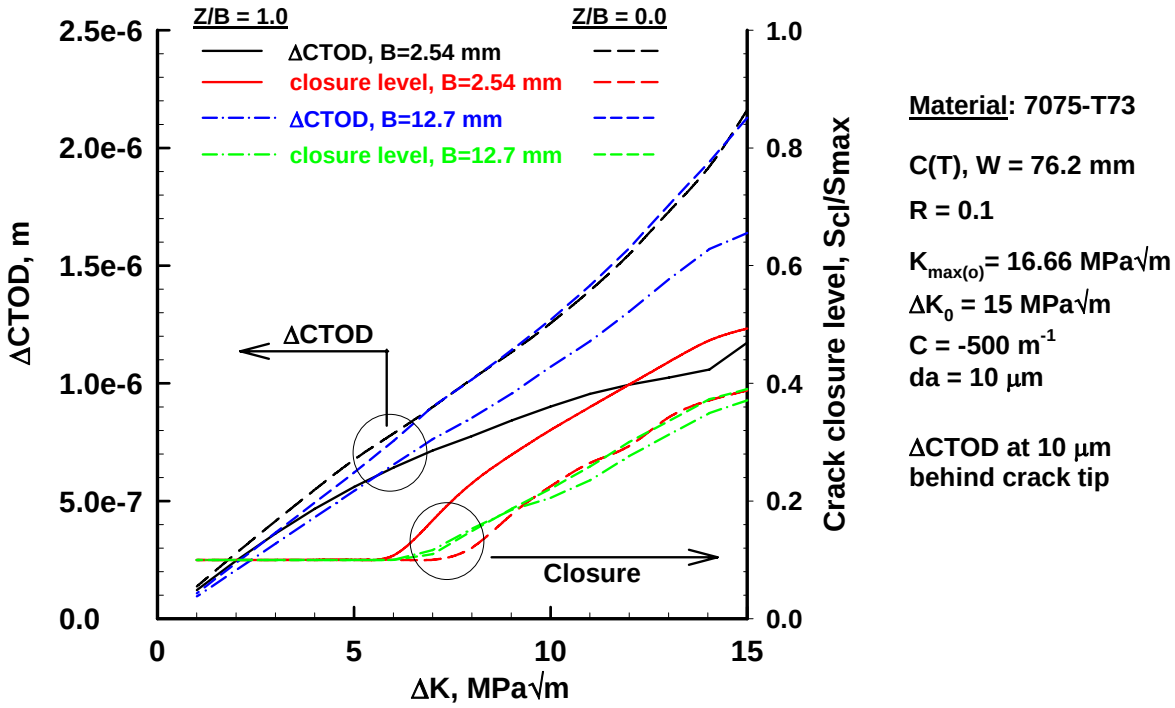

Figure 8. Variation in local ΔCTOD and closure levels with applied constant R load reduction procedure for thin and thick specimens.

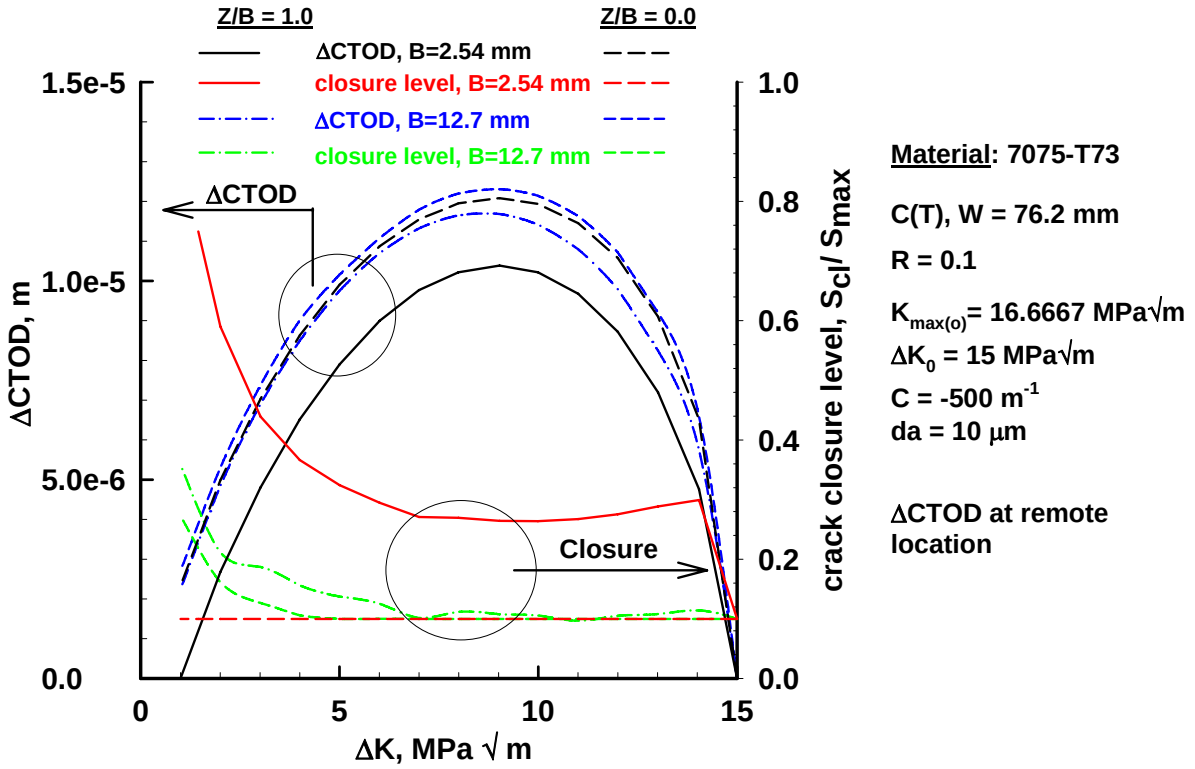

Figure 9. Variation in remote ΔCTOD and closure levels with applied constant R load reduction procedure for thin and thick specimens.

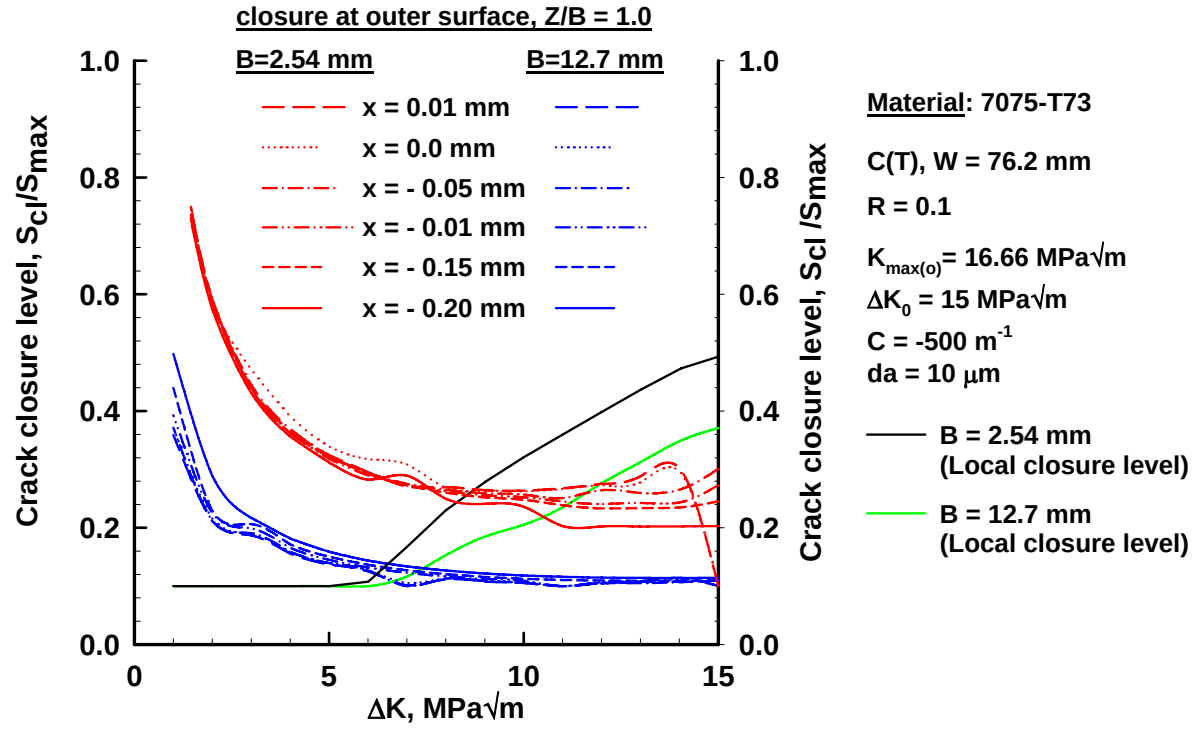

Figure 10. Comparison of variation in remote closure level on the outer surface for thin and thick specimens.